Scientific Research Publishing

Journal of Modern Physics, 2025, 16(10), 1438-1464
https://www.scirp.org/journal/jmp
ISSN Online: 2153-120X
ISSN Print: 2153-1196

Two Compartment Model of the Universe: New Source of Energy

Philip D. Houck

Division of Cardiology, Department of Medicine, Baylor Scott & White Health, Temple, TX, USA
Email: Phil@Houcktx.com

How to cite this paper: Houck, P.D. (2025) Two Compartment Model of the Universe: New Source of Energy. *Journal of Modern Physics*, **16**, 1438-1464.
https://doi.org/10.4236/jmp.2025.1610070

Received: August 17, 2025
Accepted: October 19, 2025
Published: October 22, 2025

Abstract

Unresolved aspects of quantum mechanics and cosmic energy motivated the development of a two-compartment model of the universe. Building on that foundation, the present work extends the framework by formulating equations of negentropy suggesting a potential new source of energy. The two-compartment model connects the quantum with the cosmic by mass deforming geometry of the spacetime prism. Particle masses are predicted. Star rotation in various size galaxies is calculated and is consistent with observations. The source of gluon energy in Baryons is due to extreme curvature of the spacetime prism while gravity emerges from large scale curvature of the spacetime. Converting Einstein's continuous manifold to a discrete spherical tiling prism with a thickness of Plank length adds an additional nine terms to the energy stress tensor. These terms allow properties surface tension and viscosity to explain inconsistencies. The tiling spheres of the prism generate Schrödinger waves within the prism and particles as they emerge.

Keywords

Negentropy, Geometry, Linking Quantum to the Cosmic, Particle Mass Prediction, Star Rotation, Two Compartment Universe, Replacing Manifold with a Prism

1. Introduction

Inconsistencies of current models of the universe require new concepts. Explaining observations is the goal of a two-compartment universe. The number of inconsistencies is growing. Star movement in galaxies does not conform to predictions of general relativity, soliciting dark matter as an explanation for missing mass [1] [2]. Clockwise versus counterclockwise rotation of galaxies is not predicted [3]. Fundamental forces of weak, strong, electromagnetic, and gravity have

not been united. The quantum and the cosmic seem separate without a unifying bridge. The early appearance of black holes in the young universe is unexplained [4]. The early expansion of the universe and the continued acceleration is a mystery [5]. What was the initial state that led to the big bang? What initiated the big bang? What is the future state of the universe? Cyclic or doomed? Can singularities predicted by general relativity exist? Are there many worlds predicted by quantum mechanics or only one reality [6]? What allows the property of entanglement to exist over vast distances? Corona temperature is a mystery. The structure of the universe, cosmic web is unexplained.

1.1. Theoretical Framework and Definitions

Answering the above observations and questions requires a new view of matter, energy, and entropy. The proposed hypothesis answering these questions utilizes the concept of a two-compartment model of the universe. Energy of creation is surrounded by a separate negentropy directed energy consisting of discrete tiling Planck dimensional spheres. The shell of energy represents negentropy, the means of converting energy into mass and mass into energy. Before the big bang energy was stored within the sphere and in the containing shell. No work was performed with no defined temperature. Negentropy is a dimensionless term defined as order/disorder derived in a previous paper [7] from geometry. The shell is the spacetime prism replacing Einstein's spacetime manifold.

1.2. Negentropy

$$\text{Negentropy} \quad S = -\left(\frac{1}{n^3} + \frac{3}{n^2} + \frac{3}{n}\right) \quad [7]$$

This term represents the dimensionless ratio of order/disorder of energy and mass. Entropy is the energy lost to disorder and the new source of energy, negentropy directed is energy required to maintain order. Converting energy to mass is a process of creating order and requires additional energy provided from the spacetime prism. If we consider mass generation and conversion to energy as a source and a sink, an equation of order and disorder can be computed from the thickness of the shell "t", the radius of the sphere "r" described by geometry $-\left(t^3 + 3rt^2 + 3r^2t\right)\Big/r^3$. Assigning $n = r/t$ quantize the relationship of radius to thickness of the shell establishing a dimensionless geometric rule for negentropy.

1.3. Spacetime Prism

In the beginning, before the big bang there was only energy. The energy of creation, surrounded by the negentropy directed energy contained in a spacetime prism shell. Both sources are spinning. Spacetime is not a manifold described by Riemannian geometry, a requirement in Einstein's general theory of relativity [8] [9]. Spacetime is a prism consisting of discrete, tiling spheres of energy composing the shell, approximating the thickness of Planck's length.

1.3.1. Prism versus Manifold

Adding an additional dimension, thickness of the shell, places boundary conditions of Riemann's manifold [10]. Just as in the Riemann manifold, the spacetime prism is deformed by mass. Riemann manifolds relate mass and energy to curvature also allowing infinity. Riemann cautioned in the microscopic, the extreme curved space predicted by his manifold would break down [10]. Replacing the manifold with a prism sets a boundary in the microscopic allowing calculation in the microscopic with elimination of singularities. Riemann geometry will no longer have singularities with the curvature only able to approach twice the distance of spacetime thickness. The maximum curvature of the spacetime prism occurs at these near singularities and approaches a sphere of diameter of 2 Planck lengths [11]. On macroscopic scales Riemann mass generating curvature defines gravity. On the microscopic scale, the radius, curvature, and circumference of the tiling spheres within the prism assigns quantum properties and wave functions within the media of the spacetime prism shell. The waves generated by the tiling spheres are probabilistic within the shell and exit the prism as particles. Reality is outside of the prism; probabilities exist within the prism. Entanglement occurs within spacetime and is only separated by the thickness of the prism. Entanglement is not simultaneous but less than or equal to the time calculated by the thickness of the prism divided by the speed of light.

1.3.2. Evolution of the Spacetime Prism

The property of the shell curvature induced by mass is important in understanding how the universe arose. Before creation of the universe, mass was produced in the prism shell containing energy of creation. The mass increased the prism curvature, shrinks the shell, increasing the energy density of the sphere enclosed. At a critical curvature the energy density increases above the failure threshold of the prism rupturing the spacetime prism. Pieces of the failed prism are accelerated by the impulse released by the increased energy density. The shards of the spacetime prism have rotation due to the initial rotation of the shell. The direction of rotation (counterclockwise versus clockwise [3]) depends on the initial location of the segment on the sphere and directionality of the explosive expansion. Our location within the tempest of the explosion will determine our observation of the ratio of clockwise to counterclockwise rotation of galaxies. All matters are being accelerated away from each other. The location of the original sphere of energy could be located by the ratio of clockwise to counterclockwise rotation of galaxies. The rotating shards of the prism accelerated by the explosion determine the structure of the universe, the cosmic web filaments, galaxy formation and rotation [12].

1.3.3. Properties of the Spacetime Prism

The properties of this shell convert energy into mass and mass back into energy. Like Einstein's general relativity equation derived from a manifold, mass affects curvature of the spacetime prism. Macroscopic curvature describes gravity. The extreme curvature of the microscopic is related to mass describe by additional forces. Mass produced before the big bang increases the curvature of the shell and

allows early emergence of black holes. Maximum curvature induced by mass, at the center of black holes, converts mass back into energy of the shell. As curvature of the prism approaches the cosmic, gravity emerges just as in the mass affected Riemann manifold. On the microscopic the curvature of the prism and tiling spheres are responsible for mass generation, wave function generation, electromagnetic, the weak, and the strong forces.

2. General Relativity for a Spacetime Prism

$R_{\mu\nu} - \frac{1}{2}Rg_{\mu\nu} + \Lambda g_{\mu\nu} = \kappa T_{\mu\upsilon}$ Einstein's General Relativity Equation for a manifold

Einstein's geometric manifold explaining gravity related to energies and mass is expressed as a 2nd order tensor equation. Replacing the Riemann manifold with a prism of thickness of "t" requires a 3rd order tensor due to the extra dimension. The re-formulated Riemann curvature tensor now has a fourth spatial dimension with a boundary consisting of the prism thickness. The units of the tensor change from L^{-2} to L^{-3}. The corresponding energy mass tensor now is a gradient of energy and mass across the thickness of the prism. The advantage of adding an extra dimension is micro curvature of the prism predicts quantum properties, wave equations, and macro curvature reduces to the general relativity equation. The disadvantage is the complexity in the solutions. Einstein's equation is a rank 2 symmetric tensor with 4 dimensions reducing to 10 simultaneous equations. The proposed equation will be a rank 3 symmetric tensor with 5 dimensions and a maximum of 125 components. Symmetry in uv reduces the components to 75. The proposed new equation for a prism uses a 3rd order tensor.

2.1. Modification of General Relativity

$$R_{\mu\nu\tau} - \frac{1}{2}Rg_{\mu\nu\tau} = \frac{8\pi G}{c^4}T_{\mu\nu\tau} \quad [7]$$

The cosmological component is omitted since energy can now be expressed in additional terms of the prism's 3rd order tensor. This formula may not be the final solution since the metric tensor $g_{\mu\nu}$ *along with the Ricci tensor* was introduced to conserve the order of tensors and to account for conservation of energy. The new form of the energy momentum equation is now third order and should be directly related to the Riemann tensor. The new form may be

$$R_{\mu\nu\tau} = \frac{8\pi G}{c^4}T_{\mu\nu\tau}$$

2.2. Previously Proposed Third Order Tensor

A third order tensor was previously suggested by Kaluza and Klein demonstrating the emergence of electromagnetic fields [13] [14]. Gravity is not related to the weak, strong, or the electromagnetic forces and is solely a function of curvature. The third order tensor formulation does not require a unified field theory that includes gravity. The weak, strong, and the electromagnetic are a fundamental property of the prism micro curvature. Gravity is a fundamental property of

macro curvature. Geometry is the unifying metric between the micro and cosmic.

2.3. Energy Tensor Components

T_{004} is energy density, driving mass generation via negentropy. T_{114}, T_{224}, T_{334} represent surface tension, binding quarks geometrically, analogous to gluon cohesion. $T_{\mu\nu4}$, $\mu \neq \nu$ is zero for static proton, otherwise represents shear stresses (viscosity). $T_{4\mu4}$, $T_{\mu44}$ provides cross-dimensional momentum fluxes, potentially encoding weak, strong, or electromagnetic forces. T_{444} is the shell's self-energy, contributing to intrinsic prism properties (surface tension). These forces unify quantum (binding) and cosmic (gravity, rotation) phenomena via the prism's curvature.

The following sections are not exact solutions to the proposed the higher order relativity equation. The solutions are approximate to demonstrate how curvature can determine micro and macro solutions to observe phenomena.

3. Generation of Particle Mass

Particle masses are generated by the following equation in terms of "n" the relationship between curvature and shell thickness:

$$m_n = \frac{\alpha \hbar c}{\ell_p}\left(\frac{1}{n^3}+\frac{3}{n^2}+\frac{3}{n}\right) \quad \text{where } \alpha \approx 10^{-22}.$$

m_n is particle mass associated with the radius of the particle normalized to the thickness of spacetime prism. The units are electron volts.

$\hbar c/\ell_P$ is $\hbar$ the reduced Planck constant times the speed of light divided by the Planck length. The units are in electron volts. It represents a fundamental package of energy.

n is the dimensionless ratio of radius of the particle divided by the thickness of the spacetime.

$\left(\frac{1}{n^3}+\frac{3}{n^2}+\frac{3}{n}\right)$ is -S the dimensionless negentropy directed energy. The geometry of order/disorder determines mass generation.

α is a derived constant that determines the number of tiling spheres required for mass generation and the efficiency of energy to mass conversion.

This formula predicts the mass of particles in electron volts compared to observed in Table 1.

Table 1. Predicted mass versus observed mass. (smallest n allowed $1/2\pi$).

Particle	n	Predicted Mass	Observed Mass
Top	0.18	167.5 GeV/c^2	173.4
Bottom	1	4.18 GeV/c^2	4.18
Charm	2.2	1.24 GeV/c^2	1.28
Strange	20	94.1 MeV/c^2	95
Down	400	4.49 MeV/c^2	4.8
Up	100	1.81 MeV/c^2	2.3
Electron	5000	0.36 MeV/c^2	0.5

Curvature of Particles (n)

The geometry of particles shells and cores of these particles, determined by n, as shown in Figure 1. The geometry is derived from the radius of the particle and thickness of the shell. The figures are scale adjusted. Shell role-Heavier particles (top, bottom, charm) have smaller cores and thicker shells indicating compact negentropy regions and stronger curvature. Lighter particles (up, down, electron have larger cores and thinner shells suggesting diffuse matter generation. The smaller the n the greater the deformation. A proton curvature is constructed from two up quarks and a down quark plus the cohesive energy from gluons.

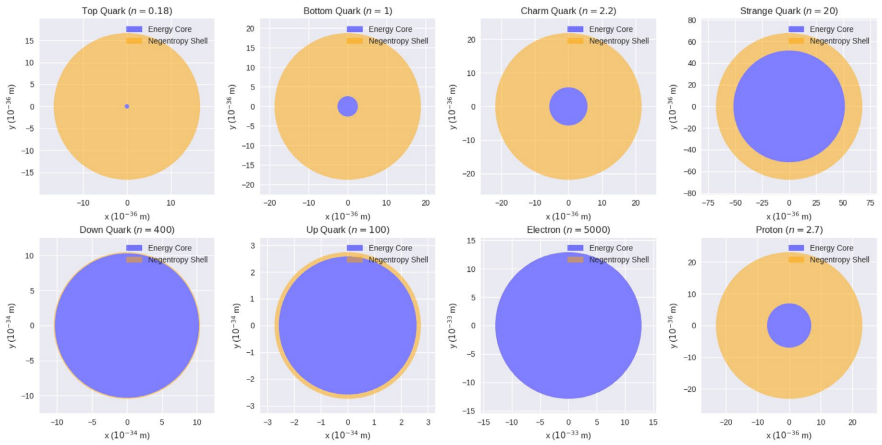

Figure 1. Energy core and negentropy shell showing curvature for various particles (n).

Neutrino masses can be predicted with $n \approx 3\times10^{6}$ suggesting extremely diffuse curvature shells—consistent with neutrinos being barely tethered to spacetime. Flavor oscillations arise from wave interference within the prism shell. Mass differences reflect slight variations in shell geometry or curvature. Entanglement and propagation are governed by the shell's thickness and refractive properties. The mass of particles predicted from this formula is graphically illustrated in Figure 2.

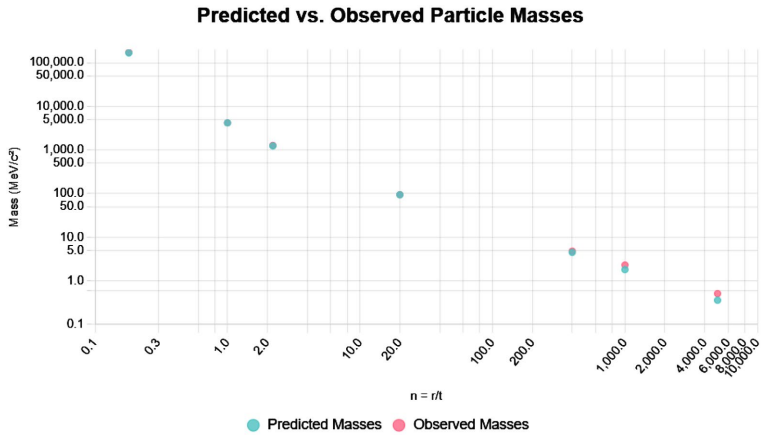

Figure 2. Plot of predicted versus observed particle masses.

4. Star Movement on the Macro-Scale

In the model of spacetime prism the rotation of stars in the galaxy depends on mass generated gravity in the core of the galaxy and additional forces generated by the spacetime prism. In addition to the force of gravity the space time prism is rotating dragging mass by surface tension, viscosity, mass generation, and other forces generated in the energy mass density tensor. At a greater radius the gravity effect of the mass of the galaxy has little effect on movement of the outer stars. In this region star movement is governed by the rotational velocity of the prism Figure 3.

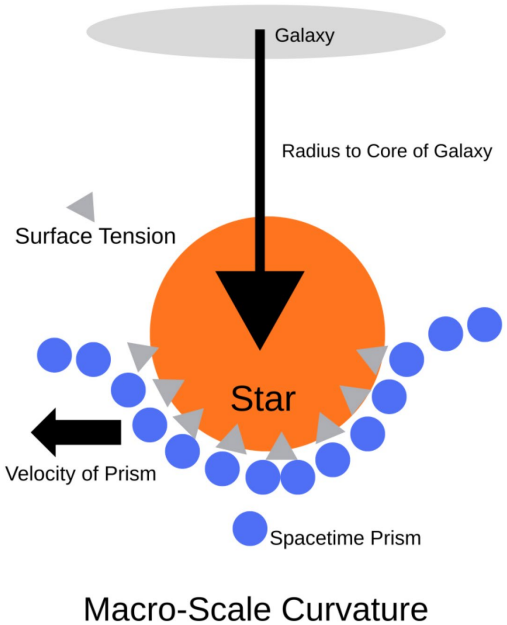

Figure 3. Surface tension of spacetime prism maintaining star velocity at distance R_d by cohesive properties of the prism (surface, viscosity, other cohesive forces, generated by the mass energy density tensor).

$$v(r)=\sqrt{\frac{GM(r)}{r}}+v(\text{prism})(r)$$

$v(r)$ is the velocity of stars in a galaxy at distance r rom the core,

G is the gravitational constant,

$M(r)=2\pi\Sigma_0 R_d^2\left[1-e^{\frac{-r}{R_d}}\left(1-\frac{-r}{R_d}\right)\right]$ the mass of the galaxy,

r is the radius from the core of the galaxy to the size of galaxy R_d,

$v(\text{prism})(r)$ is the velocity of space time prism at distance of (r) from the core of the galaxy.

For large r $v(r)=v(\text{prism})(r)$

$$v(\text{prism})(r)=\sqrt{\sigma}(r)=\sqrt{\tau\cdot\delta\cdot r}$$

Where $\sigma(r)$ represents a scaled tension field over the distance r. The units of

this field match velocity squared L^2/S^2. The magnitude of the scaled tension field assures cohesion to spacetime prism countering centripetal forces.

Deriving $\sigma(r)$ Scaled Tension over r

Viscosity, surface tension, and other forces are determined by the stress energy density tensor subjected to curvature. The surface tension τ arises from the stress-energy tensor's spatial components T_{114}, T_{224}, T_{334} acting across the prism shell. The stress-energy tensor component $T_{\mu\nu 4}$ is localized to the prism shell at $y = \ell_p$.

$$T_{\mu\nu 4} = \left[\sigma h_{\mu\nu} + \eta\left(\nabla_\mu u_\nu + \nabla_\nu u_\mu\right)\right]\delta\left(y - \ell_p\right)$$

operating in the 5D equation $R_{\mu\nu\tau} - \frac{1}{2}Rg_{\mu\nu\tau} = \frac{8\pi G}{c^4}T_{\mu\nu\tau}$

$h_{\mu\nu}$ is the projector tensor with

$h_{\mu\nu} = g_{\mu\nu} + u_\mu u_\nu$ representing the metric perpendicular to the four-velocity u^u.

η is the shear viscosity parameter, which can be associated with the calculated surface tension as a geometric analog for cohesive effects. $\eta \approx \tau$ the tensor's stress (pressure-like, kg/m·s^2 in viscosity, but kg/s^2 in surface tension) due to surface tension localized to the prism's surface via $\delta(y - \ell_p)$.

The energy density in the shell is: $T_{004} \approx 2\delta(y - \ell_p)$. Integrating over the extra dimension ($y \approx \ell_p$) gives an effective 4D stress.

The surface tension is initially modeled as:

$$\tau = \frac{\text{Energy Density}}{\text{Length Scale}} = \frac{\hbar c/\ell_p^4}{\ell_p} = \frac{\hbar c}{\ell_P^3}$$

The term ℓ_P^3 arises because the shell's thickness confines the stress and the energy density projecting onto a 2D surface. The curvature of the surface further adjusts the density so a geometric term reflecting curvature, the negentropy term, must be included to relate radius to thickness of the prism. The other necessary component is mass which also effects curvature and energy density. This component is incorporated in the dimensionless component k with the ratio mass of the galaxy/reference galaxy mass. The k is empirically determined to match rotational velocities.

The negentropy −S adjusts this density based on the prism's curvature (smaller n for higher curvature, e.g., protons; larger n for galaxies). The mass-dependent k ensures Tully-Fisher scaling ($v \propto M^{0.25}$) [15].

The final form

$$\sigma \approx \frac{\hbar c}{\ell_P^3}\left(-S\right)^k$$

$k = 1.274 - 0.0125\log_{10}\left(M_{\text{total}}/M_{\text{ref}}\right)$ $M_{\text{ref}} = 10^{11}$ M_{ref} is the mass of medium size galaxy,

$S = -\left(\frac{1}{n^3} + \frac{3}{n^2} + \frac{3}{n}\right)$ for large R_d~3/n,

$n = R_d/\ell_p$ R_d is the size of the galaxy,

The observed galaxy velocities and the velocities calculated from scaled surface tension are listed below with rotational curves for various size galaxies illustrated in Figure 4. Close to the core velocities begin to rise and flatten the farther from the core.

Small: ~106 km/s (matches dwarfs like IC 2574).

Medium: ~227 km/s (matches spirals like NGC 5055).

Large: ~261 km/s (matches giants like NGC 2903).

Milky Way: ~225 km/s (matches observed ~218 - 240 km/s).

Calculated velocities from $\sigma \approx \hbar c/\ell_p^3 \ (-S)^k$

Small $R_d = 3.086 \times 10^{19}$m n = 1.909×10^{54} $-S = 1.571 \times 10^{-54}$ $\sigma = 1 \times 10^{10}$ kg/s^2 v ≈ 100 km/s

Medium $R_d = 9.258 \times 10^{19}$m n = 5.727×10^{54} $-S = 5.239 \times 10^{-55}$ $\sigma = 4.84 \times 10^{10}$ kg/s^2 v ≈ 220 km/s

Large $R_d = 1.543 \times 10^{20}$m n = 9.545×10^{54} $-S = 3.143 \times 10^{-55}$ $\sigma = 6.2 \times 10^{10}$ kg/s^{2}v ≈ 248.9 km/s

Milky Way $R_d = 1.08 \times 10^{20}$m n = 6.682×10^{54} $-S = 4.489 \times 10^{-55}$ $\sigma = 5.071 \times 10^{10}$ kg/s^2 v ≈ 225.2 km/s

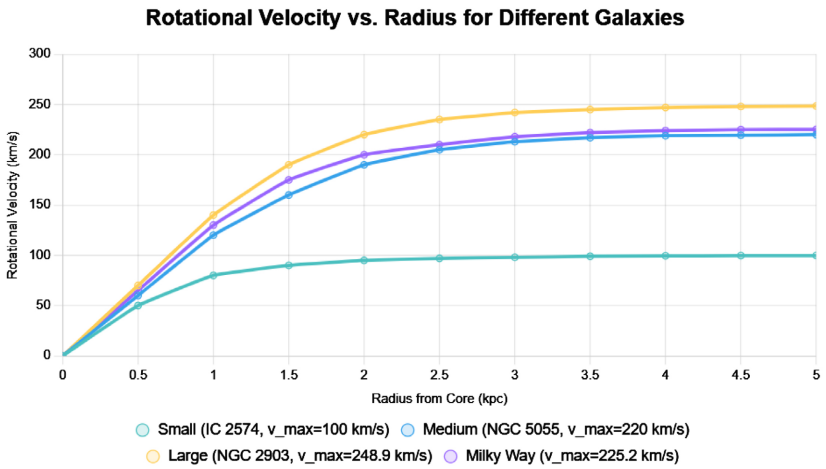

Figure 4. Rotational Curves for Different Size Galaxies demonstrating flattening of the curves away from core of the galaxy calculated from surface tension of prism.

5. Surface Tension on the Micro-Scale

Micro-curvature is illustrated in Figure 5, binding two up quarks and a down quark. The surface tension binding the quarks to form a proton is calculated using the same equation for surface tension in galaxies scaled by negentropy and mass.

Surface Tension $\sigma \approx \dfrac{\hbar c}{\ell_P^3}(-S)^k$

Where $k = 1.274 - 0.0125 \log_{10}\left(M_{2\text{up+down}} / M_{\text{proton}}\right)$

$$R_p = 0.8414 \times 10^{-15} \text{ m}$$

$$n = \frac{R_p}{\ell_p} \quad n \approx 5.206 \times 10^{19}$$

$$-S \approx 5.763\times10^{-20}$$

$$M_{2\text{up+down}} = 2\times2.3+4.8 = 9.4\ \text{MeV}/\text{c}^2$$

$$M_{\text{proton}} = 938.272\ \text{MeV}/\text{c}^2$$

$$k \approx 1.336$$

$$\sigma = 7.488\times10^{78}\times\left(5.763\times10^{-20}\right)^{1.336} \approx 1.481\times10^{53}\ \text{kg}/\text{s}^2$$

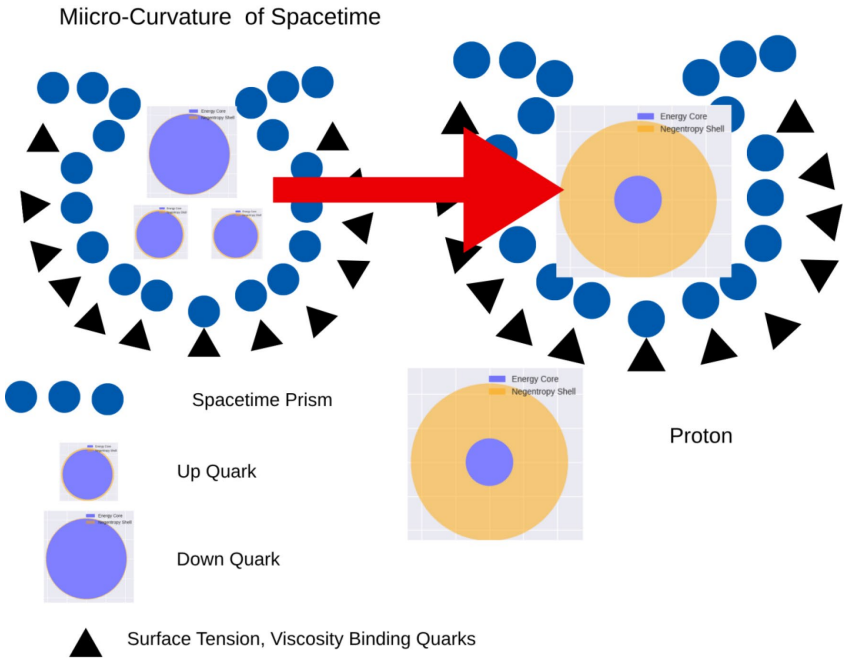

Figure 5. Counter to slight deformation of the prism seen with stars, intense curvature of the prism binds fundamental particles 2 Up + Down plus prism energy to form proton. Three particles become one establishing order.

The advantage of this geometric driven formula can be summarized:

Planck-Scale Origin: $\frac{\hbar c}{\ell_P^3} \approx 7.488\times10^{78}$ kg/s^2 is the maximum stress possible at the Planck scale, reflecting the extreme curvature of the prism shell.

Negentropy Scaling: −S quantizes the energy based on the shell's geometry $n = \frac{R}{\ell_p}$, with smaller n (high curvature) for particles like the proton, and large n (low curvature) for galaxies.

Mass-Dependent Exponent: k modulates the strength of the stress, reducing it to heavier systems (larger $M_{\text{total}}/M_{\text{ref}}$ to match physical scales (e.g., $\tau \approx 10^{53}$ kg/s^2 for protons, 10^{10} kg/s^2 for galaxies). For particles it is the ratio of unbound to bound mass. For stars the ratio of the mass of galaxy to a reference.

Stress-Energy Tensor: The tensor $T_{\mu\nu 4}$ encodes this surface tension in spatial components (e.g., T_{ii4}, replacing gluon cohesion (micro) or dark matter effects (macro) with geometric stresses localized to the shell.

6. Connecting Quantum to the Cosmic

High curvature, small scales, will describe mass generation, quantum properties, the weak, strong, and electromagnetic forces. At large scales the quantum is negligible, and curvature describes gravity. The structure of spacetime is quantified being discrete with the circumference of the tiling spheres generating wave functions of particles. Mass generation and mass conversion to energy depends on negentropy relating the spacetime radius to the thickness of the shell. The $n = r/t$ in the formula for negentropy scales from 1 reflecting the quantum to 6.682×10^{54} for the cosmic considering the radius of the Milky Way Galaxy.

The term $\hbar c/\ell_P$ represents the maximum energy density available from the spacetime curvature on the Planck scale. It's the "raw material" from which mass is generated.

Geometric Quantization via n: The polynomial $\left(\frac{1}{n^3}+\frac{3}{n^2}+\frac{3}{n}\right)$ encodes how curvature and shell geometry quantize energy into discrete particle masses. Smaller n (thicker shells) corresponds to heavier particles—more curvature, more negentropy, more mass. The prism shell's negentropy organizes energy into mass. The scaling factor α reflects the efficiency of this conversion—how much of the Planck energy is "captured" into rest mass by the number of tiling spheres and efficiency of transfer.

The mass equation suggests:

1) Mass is not intrinsic, but emergent from spacetime geometry.

2) Particles are curvature eigenstates—their mass arises from how spacetime bends at microscopic scales.

3) Energy-to-mass conversion is geometric, not field-based like the Higgs mechanism.

4) Micro curvature relates to the quantum whereas macro curvature relates to Gravity.

5) The weak strong and electromagnetic emerge from the geometry of the tiling spheres and vibrations of the spheres.

6) Gravity emerges from macro curvature of the spacetime prism.

7. Quantum Mechanics Emerge from Discrete Tiling Spheres

Schrödinger's wave equation was developed to explain the wave-like behavior of matter [16]. The circumference of each tiling sphere of the prism is the perfect media for generating waves. Waves can be influenced by the spin of these spheres and quantum properties are imposed by the radius circumference, and requirement of being bound to the surface. The shell's curvature (via negentropy S) generates a potential $V(r)$, modeled as a delta function at the Planck scale, binding waves like a quantum well. The wave function is separated into radial $R(r)$ and angular $Y_q^{\ell}(\theta,\varphi)$ parts, leading to the radial equation, with the angular momentum term arising from the spheres' discrete rotations.

7.1. Quantization from Tiling Spheres

Waves traveling in the shell must "fit" the discrete geometry, like standing waves on a closed loop. The model quantizes the circumference to integer multiples of a fundamental wavelength $\lambda \approx \ell_P$

$$C = 2\pi r = q\lambda \quad \text{with} \quad q = 1, 2, 3, \cdots \lambda \approx \ell_p \quad \text{then} \quad r = q\ell_p / 2\pi$$

This quantization imposes boundary conditions on the wave function, discretizing positions, momenta, and energies. The tiling spheres' periodicity (lattice-like structure) introduces angular momentum quantization, as waves "twist" around the spheres, leading to the centrifugal term in the wave equation. The negentropy S ties to this via n

$$n = \frac{r}{\ell_p} = q/2\pi \quad \text{for} \quad q = 1 \quad \text{the lowest} \quad n = 0.16$$

$S = -\left(\frac{1}{n^3} + \frac{3}{n^2} + \frac{3}{n}\right)$ quantizes the energy organization in the shell, with smaller n (tighter curvature) for heavier particles.

7.2. Wave Function and Separation of Variables

The full wave function $\psi(r, \theta, \varphi)$ in spherical coordinates (fitting the spherical tiling) is separated as:

$$\psi(r, \theta, \phi) = R(r) Y_q^{\ell}(\theta, \phi)$$

with ℓ the angular quantum number (quantized due to the spheres' symmetry) and q the magnetic quantum number ($-\ell \le q \le \ell$).

The Schrödinger equation is:

$$-\frac{\hbar^2}{2m}\nabla^2\psi + V(r)\psi = E\psi$$

Substituting the separated form, the Laplacian ∇^2 separates into radial and angular parts:

$$\nabla^2 = \frac{1}{r^2}\frac{\partial}{\partial r}\left(r^2 \frac{\partial}{\partial r}\right) + \frac{1}{r^2 \sin\theta}\frac{\partial}{\partial \theta}\left(\sin\theta \frac{\partial}{\partial \theta}\right) + \frac{1}{r^2 \sin\theta}\frac{\partial^2}{\partial \Phi^2}$$

The angular part gives the eigenvalue $-\ell(\ell+1)$ for Y_q^{ℓ}, leading to the radial equation for $R(r)$:

$$-\frac{\hbar^2}{2m}\left(\frac{\mathrm{d}^2}{\mathrm{d}r^2} + 2\frac{\mathrm{d}}{r\mathrm{d}r}\right)R(r) + \frac{\hbar^2}{2mr^2}\ell(\ell+1)R(r) + V(r)R(r) = ER(r)$$

The potential V(r) models the prism shell's boundary, approximated as a delta function at the Planck scale: $V(r) \approx \left(\frac{\hbar^2}{2m}\right) Q\delta(r - \ell_p) V(r)$, where Q is a constant related to shell stiffness or curvature. Q is non dimensional scaling term consisting of negentropy term and exponent k relating to bound versus unbound mass.

Q is related to $\left(-\frac{1}{\left(r/\ell_p\right)^3}+\frac{3}{\left(r/\ell_p\right)^2}+\frac{3}{r/\ell_p}\right)^k$ where $k = 1.274 - 0.0125 \log_{10}(M_{\text{unbound mass}}/M_{\text{bound mass}})$.

$\hbar^2/2$ m has units of energy × length^2, δ has 1/length, so V has energy units.

8. Is Negentropy Energy?

The physicist Erwin Schrödinger (1944), "What Is Life? The Physical Aspect of the Living Cell" introduced the concept of negative entropy-(*entropy*) = $k\log(1/D)$ [17]. Where k is Boltsmann's constant and D is an atomistic measure of disorder. This form is in Joules/Kelvin and is dependent on temperature. It represents the energy to maintain order. He chose to study biology to find new physics. Entropy and Negentropy over a lifetime are very evident. Lower body temperature predicts longevity, greater complexity with an additional Y chromosome shortens lifespan. Negentropy is evident when two cells become one at the time of conception [18]-[20]. Entropy eventually dominates with organ failures of aging, and the body reverts to room temperature. Schrödinger was correct, if negentropy has a role in biology it must have a role in general physics. The Negentropy term −S is non-dimensional just as in information theory. Negentropy directs the energy in the prism to produce particles adding order. To do so it has access to energy. Is negentropy energy or a director of energy? The prism is the source.

9. Implications of a 2-Compartment Universe

1) The quantum and the cosmic are bridged by geometry determined by negentropy and the space time prism.

2) Star movement in galaxies is predicted without dark matter or dark energy by considering the property of surface tension, and cohesive properties of the spacetime prism.

3) Particle masses are predicted by negentropy formula $m_n = \frac{\alpha\hbar c}{\ell_p}\left(\frac{1}{n^3}+\frac{3}{n^2}+\frac{3}{n}\right)$ where $\alpha \approx 10^{-22}$.

4) Clockwise versus counterclockwise rotation of galaxies occurred when the prism shell failed, sending shards of the prism rotating into the future universe.

5) Fundamental forces of weak, strong, electromagnetic, emerge from extreme curvature of the prism and gravity emerge from macro-curvature.

6) The early appearance of black holes in the young universe is related to mass generation by spacetime prism before the big bang.

7) The early expansion of the universe and the continued acceleration was when the curvature generated mass compressed the energy of creation to the failure limit of the prism container.

8) The initial state of the universe that led to the big bang was a sphere of energy surrounded by a spacetime prism of tiling spheres of negentropy.

9) The universe is cyclic converting energy of mass back into negentropy.

10) The prism model eliminates singularities and replaces them with very large numbers.

11) Probabilities exist within the prism and particles emerge from the prism into one reality.

12) Entanglement is not simultaneous, separated by a very small-time interval calculated as the speed of light divided by the thickness of the prism.

13) The energy of gluons holding quarks together in baryons is emergent from the tiling spheres of the spacetime prism.

14) Negentropy and the spacetime prism is the new source of energy.

10. Caveats

1) Particle masses predicted approximated masses observed. Other forces emerging from the third order energy mass density tensor will have influence refining predictions.

2) The author is a cardiologist with experience in negentropy related biology. My goal is to extend these notions to physics and extend the second law of thermodynamics to include order.

3) Solutions presented are only an approximation. Solving 75 simultaneous equations remains elusive to the author.

4) Energy is in the prism. Can it be harnessed? The same question was asked of the atom.

11. Conclusions

A two-compartment model of the universe refines Einstein's notion of General Relativity by replacing spacetime manifold with a spacetime prism. The quantum and cosmic are united thru geometry of spacetime prism. Curvature the main driver of geometry is related to negentropy and prism deformed by mass. The price of this notion is increasing the order of the tensor solution of Einstein's equation from 2 to 3 adding additional terms. The additional terms describe surface tension, viscosity, and binding forces of particles. Surface tension of the prism supplies the forces explaing star velocites at the peiphery of galaxies and the binding energy of gluons. Negentropy $-S = (1/n^3 + 3/n^2 + 3/n)$ is the director of new source of energy stored in the spacetime prism. It is proposed that the second law of thermodynamics should include the concept of maintaining order. The negentropy geometric equation was derived from source and sinks of mass production occurring on a sphere of energy contained by a shell of a spacetime prism. The inconsistencies listed in the introduction are reconciled with the two-compartment model. Further efforts are required to develop these concepts. An **Appendix** is included to further refine topics listed below:

A.1 Prism Curvature;

A.2 Derivation of Action Lagrangian;

A.3 Comparison of Maximal curvature in the Two -Compartment Model versus String Theory;

A.4 Weak Field Limit Analysis of the Energy-Mass Density Tensor in the Two-Compartment Model Compared to General Relativity;

A.5 Predictions of Corona Temperature compared to Observations.

Conflicts of Interest

The author declares no conflicts of interest regarding the publication of this paper.

References

[1] Rubin, V.C., Thonnard, N. and Ford Jr., W.K. (1980) Rotational Properties of 21 SC Galaxies with a Large Range of Luminosities and Radii, from NGC 4605 (R = 4 kpc) to UGC 2885 (R = 122 kpc). *The Astrophysical Journal*, **238**, 471-487. https://doi.org/10.1086/158003

[2] Rubin, V.C. (1983) Dark Matter in Spiral Galaxies. *Scientific American*, **248**, 96-108. https://doi.org/10.1038/scientificamerican0683-96

[3] Shamir, L. (2024) Galaxy Spin Direction Asymmetry in JWST Deep Fields. *Publications of the Astronomical Society of Australia*, **41**, e038. https://doi.org/10.1017/pasa.2024.20

[4] Maiolino, R., Scholtz, J., Witstok, J., Carniani, S., D'Eugenio, F., de Graaff, A., *et al.* (2024) A Small and Vigorous Black Hole in the Early Universe. *Nature*, **627**, 59-63. https://doi.org/10.1038/s41586-024-07052-5

[5] Solà Peracaula, J. (2022) The Cosmological Constant Problem and Running Vacuum in the Expanding Universe. *Philosophical Transactions of the Royal Society A*: *Mathematical*, *Physical and Engineering Sciences*, **380**, Article ID: 20210182. https://doi.org/10.1098/rsta.2021.0182

[6] Everett, H., Wheeler, J.A., DeWitt, B.S., Cooper, L.N., Van Vechten, D., Gra-ham, N., DeWitt, B. and Neill, G.R. (1973) The Many-Worlds Interpretation of Quantum Mechanics. Princeton University Press.

[7] Houck, P.D. (2024) Star Movement Is Not Predicted Two-Compartment Model of the Universe. *Journal of Modern Physics*, **15**, 1679-1689. https://doi.org/10.4236/jmp.2024.1511073

[8] Einstein, A. (1905) Zur Elektrodynamik bewegter Körper. *Annalen der Physik*, **322**, 891-921. https://doi.org/10.1002/andp.19053221004

[9] Einstein, A. (1917) On the Special and General Theory of Relativity. *CPAE* (*English Translation*), **6**, 247-420.

[10] Riemann, B. (2016) On the Hypotheses Which Lie at the Bases of Geometry. Birkhäuser Cham.

[11] Planck, M. (1899) Natuerliche Masseinheiten. Der Königlich Preussischen Akademie der Wissenschaften.

[12] Zarattini, S. and Aguerri, J.A.L. (2025) Galaxy Transformation across the Cosmic Web: Evolution of Stellar Colours and Star Formation Rates in Filaments. *Astronomy & Astrophysics*, **698**, A196. https://doi.org/10.1051/0004-6361/202453053

[13] Kaluza, T. (1921) Zum unitätsproblem der physik. arXiv: 1803.08616.

[14] Klein, O. (1991) Quantum Theory and Five-Dimensional Relativity Theory. In: Ekspong, G., Ed., *The Oskar Klein Memorial Lectures*, World Scientific, 67-80. https://doi.org/10.1142/9789814368728_0006

[15] Tully, R.B. and Fisher, J.R. (1977) A New Method of Determining Distances to Gal-

axies. *Astronomy and Astrophysics*, **54**, 661-673.

[16] Schrödinger, E. (1926) Quantisierung als Eigenwertproblem. *Annalen der Physik*, **384**, 361-376. https://doi.org/10.1002/andp.19263840404

[17] Schrödinger, E. (1944) What Is Life? The Physical Aspect of the Living Cell. Based on Lectures Delivered under the Auspices of the Dublin Institute for Advanced Studies at Trinity College.

[18] Houck, P.D. (2014) Should Negative Entropy Be Included in the Fundamental Laws of Biology? *OA Biology*, **2**, Article No. 7.

[19] Houck, P.D. (2020) Making Drug Discovery More Efficient Applying Statistical Entropy to Biology. *Journal of Modern Physics*, **11**, 1969-1976. https://doi.org/10.4236/jmp.2020.1112124

[20] Houck, P.D. (2025) Entropy and the Lymphatic System, a New Model with Therapeutic Potential. *Global Journal of Medical Research*, **25**, 27-38. https://doi.org/10.34257/gjmrbvol25is1pg27

Appendix A.1 Prism Curvature

Geometry of the Tiling Spheres

Diameter of Tiling Spheres: Given as ℓ_P, the radius of each sphere is $\frac{\ell_p}{2} \approx 8.081145 \times 10^{-16}$

Tiling Assumption: The prism is a thin shell (thickness $t \approx \ell_P$ tiled by these spheres without gaps, forming a lattice. In 3D Euclidean space, the densest packing of spheres is the face-centered cubic or hexagonal close-packed arrangement, achieving a packing fraction of $\frac{\pi}{3\sqrt{2}} \approx 0.7405$. However, in the 5D prism, the extra dimension (index 4) may allow a higher effective density due to compactification or discrete stacking along y.

Curvature Scale: The curvature is inversely related to the scale of the tiling. The smallest radius ($\ell_P/2$) sets the fundamental length scale, suggesting curvature scales as $1/(\ell_P/2)^2 = 4/\ell_P^2$

Curvature Definition

In general relativity, the Ricci scalar R (units m^{-2}) represents the intrinsic curvature of spacetime. For a discrete lattice, the curvature is approximated by the discrete Laplacian or the geodesic deviation over the tiling scale. The maximal curvature occurs where the tiling spheres are most tightly packed, *i.e.*, at the Planck scale, where the prism's thickness and sphere diameter coincide.

The model uses a 5D framework, so the relevant curvature includes the third-order term $R_{\mu\nu\tau}$, which couples to $T_{\mu\nu\tau}$. The Ricci scalar in 5D ($R^{(5)}$) is the trace of the 5D Ricci tensor, but the prism's discrete nature suggests focusing on the local curvature induced by the tiling.

Negentropy and Stress-Energy Contribution

The negentropy $S = -\left(\frac{1}{n^3} + \frac{3}{n^2} + \frac{3}{n}\right)$, with $n = R/\ell_P$, quantifies order. For the maximal curvature, consider the smallest R, the radius of a single tiling sphere ($R \approx \frac{\ell_p}{2}$):

$$n = \frac{\ell_p}{2\ell_p} = \frac{1}{2} \quad S = -\left(\frac{1}{\left(\frac{1}{2}\right)^3} + \frac{3}{\left(\frac{1}{2}\right)^2} + \frac{3}{\left(\frac{1}{2}\right)}\right), \quad S = -(8+12+6) = -26 \quad -S = 26$$

The surface tension $\tau \approx \frac{\hbar c}{\ell_p^3}(-S)^k$ with $k \approx 1.274$ for minimal systems) contributes to $T_{\mu\nu\tau}$

For $k = 1.274$

$$\tau \approx \left(7.488 \times 10^{78}\right) \times 1.2 \times 10^3 \approx 9.0 \times 10^{81}\ \mathrm{kg/s^2}$$

This extreme tension reflects the maximal stress t the Planck scale, feeding into $T_{\mu\nu\tau} \sim \tau/\ell_p \sim 10^{116}$ kg·m^{-2}·s^{-2}.

Curvature from Tensor Coupling

The field equation $R_{\mu\nu\tau} = \kappa T_{\mu\nu\tau}$ relates curvature to the tensor. The maximal $T_{\mu\nu\tau}$ occurs where the tiling density is highest, *i.e.*, $n = 1/2$. The curvature $R_{\mu\nu\tau}$ has units m^{-3} and $\kappa \sim 8\pi G_5/c^4$ (units kg^{-1}·m^3·s^2).

To find the scalar curvature $R^{(5)}$, trace over indices. Assuming isotropy at maximal density, R $R_{\mu\nu\tau} \sim R/\ell_p^3$ (projecting 5D curvature to 3D scale), the maximal $R \sim \ell_p^{-2} \cdot (-S) \cdot \kappa T \sim 10^{-26}$ kg^{-1}·m^3·s^2 (estimated from 5D compactification):

$$R_{\max} \approx 2.2 \times 10^{211} \text{ m}^{-2}$$

This is an upper bound, as κ and tensor projection need precise 5D calibration. The standard Planck-scale curvature $1/\ell_p^2 \approx 3.8 \times 10^{69}$ m^{-2} is exceeded due to negentropy amplification.

Maximal Curvature Constraint

The tiling spheres' discreteness limits curvature: Beyond $\ell_P/2$, quantum gravity effects (e.g., string theory) or prism rupture (containment vessel) may cap it. The maximal physical curvature is thus tied to the densest packing, where $R_{\max} \sim 10^{69}$ - 10^{211} m^{-2} as a practical limit (matching Planck curvature without excessive negentropy boost.

Curvature Summary

The maximal curvature of the spacetime prism, considering tiling spheres with a diameter of the Planck length $\ell_P \approx 1.616229 \times 10^{-35}$, is approximately:

$$R_{\max} \sim 4\ell_p^2 \cdot (-S)_{\max} \approx 1.58 \times 10^{71} \text{ m}^{-2} \cdot$$

This assumes a conservative negentropy scaling (n = 1/2, −S = 26) without full 5D tensor amplification. The upper bound, including tensor and coupling effects, may reach 10^{211} m^{-2}, but the Planck-scale limit $1/\ell_p^2 \approx 3.8 \times 10^{69}$ m^{-2} is likely the physical maximum due to discreteness constraints.

Appendix A.2 Derivation of Action Lagrangian

Derivation of the Action Lagrangian

Standard Einstein-Hilbert Action as a Starting Point

In 4D general relativity, the action S_a is given by the Einstein-Hilbert Lagrangian:

$$S_a = \int \mathcal{L}_{EH} \sqrt{-g}\, \mathrm{d}^4 x, \quad \mathcal{L}_{EH} = c^4 R/16\Pi G$$

where:

R is the Ricci scalar,

g is the determinant of the metric $g_{\mu\nu}$,

G is the gravitational constant,

c is the speed of light.

This action describes the geometry of spacetime coupled to a second-order stress-energy tensor $T_{\mu\nu}$ via the Einstein field equations $R_{\mu\nu\tau} - \frac{1}{2} R g_{\mu\nu\tau} = \frac{8\pi G}{c^4} T_{\mu\nu\tau}$.

In the two-compartment model, the manifold is replaced by a 5D prism with a third-order tensor $T_{\mu\nu\tau}$, sourced in $R_{\mu\nu\tau} = \kappa T_{\mu\nu\tau}$ (or the modified form $R_{\mu\nu\tau} - \frac{1}{2} R g_{\mu\nu\tau} = \kappa T_{\mu\nu\tau}$), where κ is a 5D coupling constant analogous to $8\pi G/c^4$.

Extension to 5D Prism Geometry

The prism introduces a fifth dimension (index $\tau = 4$) corresponding to its thickness ($\sim \ell_P$), tiled by spheres with negentropy-driven energy. The action must generalize to 5D, integrating over x_μ (0 - 3) and y (4th spatial coordinate):

$$S_a = \int \mathcal{L} \sqrt{-g^{(5)}} \, \mathrm{d}^{(5)} x$$

where $g^{(5)}$ is the 5D metric determinant, and the Lagrangian $\mathcal{L}$ includes contributions from the prism's curvature and the third-order tensor.

The 5D Ricci tensor $R^{(5)}_{\mu\nu\tau}$ (from the 5D metric) and the third-order curvature $R_{\mu\nu\tau}$ (specific to the prism's discrete structure) replace the 4D R. The model suggests $R_{\mu\nu\tau}$ encodes additional degrees of freedom (e.g., surface tension $\tau \approx \frac{\hbar c}{\ell_p^3} (-S)^k$, viscosity $\eta \approx \tau$, so the Lagrangian should couple $R_{\mu\nu\tau}$ to $T_{\mu\nu\tau}$.

Defining the Lagrangian

The action Lagrangian $\mathcal{L}$ should consist of:

Gravitational Term: A 5D curvature scalar or third-order curvature term, generalizing R.

Matter Term: The third-order stress-energy tensor T, representing energy-mass density from tiling spheres.

Negentropy Contribution: S as a geometric order parameter, modulating the tensor's strength.

Given the prism's discrete nature, the Lagrangian is proposed as: Two-Compartment Action Lagrangian

Given the prism's discrete nature, the Lagrangian is proposed as:

$$\mathcal{L} = \frac{c^4}{16\Pi G_5} R^{(5)} + \kappa T_{\mu\nu\tau} R^{\mu\nu\tau} + \lambda (-S) T_{\mu\nu\tau} T^{\mu\nu\tau}$$

where:

$R^{(5)}$: 5D Ricci scalar, with G_5 the 5D gravitational constant (related to 4D G via compactification, $G_5 \sim G/\ell_P$.

$R^{\mu\nu\tau}$: Dual of the third-order curvature tensor, contracted with $T_{\mu\nu\tau}$ to enforce field equations.

κ: Coupling constant, $\kappa \sim 8\pi G_5 / c^4$, adjusted for 5D.

λ: A dimensionless constant scaling negentropy's effect on tensor self-interaction.

$-S = \left(\frac{1}{n^3} + \frac{3}{n^2} + \frac{3}{n}\right)$: Negentropy, with $n = R/\ell_P$ (radius of the system, e.g., proton or galaxy, over Planck length).

Field Equations from Variation

Varying the action $S_a = \int \mathcal{L}\sqrt{-g^{(5)}}\,\mathrm{d}^{(5)}x$ with respect to the 5D metric $g^{(5)}_{\mu\nu}$

$$\frac{\delta\left(\mathcal{L}\sqrt{-g^{(5)}}\right)}{\delta g^{(5)}_{\mu\nu}} = 0$$

Physical Interpretation

Gravitational Term: $R^{(5)}$ governs large-scale curvature (e.g., galaxy rotation).

Tensor Coupling: $T_{\mu\nu\tau}R^{\mu\nu\tau}$ links prism geometry to forces (e.g., surface tension replacing dark matter).

Negentropy Term: $(-S)T_{\mu\nu\tau}T^{\mu\nu\tau}$ quantifies order, driving particle masses $m_n = \frac{\alpha\hbar c}{\ell_p}(-S)$ and energy transport (e.g., coronal heating).

Summary of Action Lagrangian

The action Lagrangian for the energy-mass density tensor in the two-compartment model is:

$$\mathcal{L} = \frac{c^4}{16\Pi G_5}R^{(5)} + \kappa T_{\mu\nu\tau}R^{\mu\nu\tau} + \lambda(-S)T_{\mu\nu\tau}T^{\mu\nu\tau}$$

where:

$R^{(5)}$ The 5D Ricci scalar,

$T_{\mu\nu\tau}$ is the third-order stress-energy tensor (units $\mathrm{kg\cdot m^{-2}\cdot s^{-2}}$),

$R^{\mu\nu\tau}$ is the dual third-order curvature,

$\kappa \sim 8\pi G_5/c^4$ (units $\mathrm{kg^{-1}\cdot m^3\cdot s^2}$),

λ is a coupling constant (units $\mathrm{kg^{-1}\cdot m^4\cdot s^2}$),

$S = -\left(1/n^3 + 3/n^2 + 3/n\right)$ is the negentropy (dimensionless), with $n = R/\ell_P$.

Appendix A.3 Comparison of Maximal Curvature in the Two-Compartment Model versus String Theory

In the two-compartment model, the maximal curvature of the spacetime prism—limited by the discrete tiling spheres with diameter equal to the Planck length ($\ell_p \approx 1.616 \times 10^{-35}$ is derived from the smallest geometric scale and negentropy amplification. As calculated previously, it is approximately $R_{max} \sim 1.58 \times 10^{71}\ \mathrm{m^{-2}}$ (conservative, with n = 1/2 and −S = 26), or up to $10^{211}\ \mathrm{m^{-2}}$ with full tensor coupling effects, but practically capped at the Planck curvature $1/\ell_p^2 \approx 3.8 \times 10^{69}\ \mathrm{m^{-2}}$ due to discreteness and potential shell rupture (analogous to the Big Bang in the model). This curvature arises from the prism's third-order tensor $R_{\mu\nu\tau} = \kappa T_{\mu\nu\tau}$

where high micro-curvature (small n) generates particle masses and forces, replacing continuous manifolds with a tiled shell.

String theory, in contrast, treats spacetime as a 10- or 11-dimensional continuum (e.g., in superstring or M-theory frameworks), where strings (fundamental 1D objects) vibrate to produce particles and forces. The maximal curvature in string theory is typically associated with the string scale or Planck scale, beyond which quantum gravity effects dominate, and classical general relativity breaks down. The characteristic curvature scale is $1/\ell_s^2$, where the string length ℓ_s is often on the order of ℓ_p (or slightly larger, $\ell_s \sim 10^{-34}$ - 10^{-35} m in some models), yielding $R_{\max} \sim 1/\ell_s^2 \approx 10^{68}$ - 10^{70} m^{-2}. At these scales, spacetime becomes "fuzzy" due to string excitations, avoiding singularities (e.g., in black hole interiors), and T-duality or mirror symmetry limits extreme curvatures by relating small radii to large ones.

Key Similarities

Planck-Scale Dominance: Both models are capped near the Planck curvature $\sim 10^{69}$ m^{-2}, where quantum effects prevent infinite curvature (singularities). In the two-compartment model, discreteness of tiling spheres eliminates singularities, like how strings "smear" spacetime at ℓ_s.

Unification of Forces: The prism's tensor unifies gravity (macro-curvature) with quantum forces (micro-curvature, e.g., replacing gluons), echoing string theory's unification via vibrational modes producing gravitons, gauge bosons, and matter particles.

Dimensional Compactification: The prism's extra dimension (thickness ℓ_P) is compactified, akin to string theory's 6 - 7 compact dimensions (Calabi-Yau manifolds) at the Planck scale, generating EM-like fields (as in Kaluza-Klein extensions in both).

Key Differences

Discrete vs. Continuous Structure: The two-compartment model's prism is fundamentally discrete (tiling spheres), leading to a "quantized" curvature limit tied to sphere packing density (e.g., face-centered cubic packing fraction ~0.74 constrains maximal "bending"), potentially allowing slightly higher effective curvatures (~10^{71} m^{-2}) via negentropy amplification. String theory is continuous at larger scales but introduces fuzziness via string world sheets, with curvature resolved at $\alpha' = \ell_s^2/4\pi$ α' (Regge slope parameter), typically capping at ~10^{70}m^{-2} without discrete caps.

Curvature Amplification: The model's negentropy −S and tensor coupling can amplify curvature beyond the base Planck value (up to 10^{211} m^{-2} theoretically), driven by geometry and order/disorder. String theory curbs this via higher-order corrections (e.g., R^4 terms in the effective action), preventing divergences but without explicit amplification factors like −S.

Dimensionality and Forces: The model uses 5D with a third-order tensor to emerge forces (e.g., surface tension replacing dark matter), while string theory requires 10D/11D, with branes and fluxes for force unification. String theory's max-

imal curvature often relates to black brane horizons or AdS throats (~10^{60} - 10^{70} m^$^{-2}$ in warped throats), lower than the model's amplified limit but similar in base scale. Comparison is in Table A1.

Table A1. Quantitative comparison table.

Aspect	Two-Compartment Model	String Theory
Base Scale	$1/\ell_P^2 \approx 3.8\times10^{69}$ m^{-2}	$1/\ell_s^2 \approx 10^{68}$ - 10^{70} m^{-2} ($\ell_s \sim \ell_P$)
Amplified Max	~1.58×10^{71} m^{-2} (negentropy S); up to 10^{211}m^{-2} with tensor	~10^{70} m^{-2}; limited by α' corrections, no explicit amplification
Limiting Mechanism	Discrete tiling spheres; shell rupture at critical n	String excitations/fuzziness; T-duality (small radii - large)
Physical Implications	Unifies forces via prism geometry; predicts masses/rotation without dark matter	Unifies via string modes; resolves singularities; predicts extra dimensions/branes

The two-compartment model's curvature is comparable in base scale to string theory's but potentially higher due to negentropy-driven amplification, offering a discrete alternative to string fuzziness for quantum gravity resolution. Both avoid singularities at ~10^{70} m^{-2}, but the model's third-order tensor provides unique predictions (e.g., coronal heating via EM conduits).

Appendix A.4 Weak Field Limit Analysis of the Energy-Mass Density Tensor in the Two-Compartment Model Compared to General Relativity

The two-compartment model's third-order stress-energy tensor $T_{\mu\nu\tau}$ (in 5D spacetime, with $\tau = 4$ for the prism thickness) is sourced in the field equation $R_{\mu\nu\tau} = \kappa T_{\mu\nu\tau}$ (or the variant $R_{\mu\nu\tau} - \frac{1}{2} R g_{\mu\nu\tau} = \kappa T_{\mu\nu\tau}$, where $R_{\mu\nu\tau}$ is a third-order curvature tensor derived from the prism geometry. To analyze the weak-field limit, we linearize the equations around a flat 5D metric and compactify the extra dimension to obtain an effective 4D theory, comparing it to standard general relativity. This approach draws from Kaluza-Klein theory, as the model cites Kaluza-Klein for emerging electromagnetic fields, but extends it with the third-order tensor for additional forces (e.g., surface tension replacing dark matter).

The weak-field limit assumes small perturbations (e.g., gravitational fields much weaker than c^2/r, like in the solar system or galaxy outskirts), reducing nonlinear equations to linear Poisson-like forms. In general relativity, this yields Newtonian gravity; in the model, it should recover general relativity plus corrections from negentropy $S = -\left(\frac{1}{n^3} + \frac{3}{n^2} + \frac{3}{n}\right)$ and the extra dimension.

Weak-Field Limit in Standard General Relativity (4D Baseline)

In general relativity, the metric is perturbed as $g_{\mu\nu} = \eta_{\mu\nu} + h_{\mu\nu}$ where $|h_{\mu\nu}| \ll 1$,

$\eta_{\mu\nu} = \text{diagonal}(1,-1,-1,-1)$ is the Minkowski metric, and we use the harmonic gauge $\partial^{\mu}\bar{h}_{\mu\nu} = 0$, $\partial^{\mu}\bar{h}_{\mu\nu} = h_{\mu\nu} - 1/2\,\eta_{\mu\nu}h$,

The linearized Einstein equations are:

$$\Box \bar{h}_{\mu\nu} = -\left(16\pi G/c^4\right)T_{\mu\nu}$$

where $\Box = \partial^2 t/c^2 - \nabla^2$ is the d'Alembertian. For static, low-velocity sources (non-relativistic limit, $T_{00} \approx \rho c^2$, other components small):

$$\nabla^2 h_{00} = \left(8\pi G/c^2\right)\rho, \quad h_{00} = -2\Phi/c^2$$

recovering Newton's law $\nabla^2\Phi = 4\pi G\rho$ with Φ the Newtonian potential.

Weak-Field Limit in the Two-Compartment Model (5D with Third-Order Tensor)

The model is in 5D (indices A, B, C = 0 - 4), with metric $g^{(5)}_{AB} = \eta^{(5)}_{AB} + h_{AB}AB^{(5)}$, $\eta^{(5)}_{AB} = \text{diagonal}(1,-1,-1,-1,-1)$, and the extra dimension y (compactified to ~ ℓ_P). The third-order curvature $R_{\mu\nu\tau}$ is non-standard (not the usual rank-4 Riemann) but interpreted as a contracted Ricci-like tensor with extra index for prism thickness. From Kaluza-Klein analogies we compactify y, reducing to effective 4D fields.

Linearization:

Perturb the 5D metric: $h^{(5)}_{AB} \ll 1$.

The 5D Ricci tensor linearizes as

$R^{(5)}_{AB} = -1/2\,\Box^{(5)}h^{(5)}_{AB} + 1/2\,\partial_A\partial_C h^{(5)}_{CB} + 1/2\,\partial_B\partial_C h^{(5)}_{CA} - 1/2\,\partial_A\partial_B h^{(5)}_{CC}$ (in gauge).

The model's third order $R_{\mu\nu\tau}$ may be $R_{\mu\nu\tau} = \partial_{\tau}R^{(4)}_{\mu\nu}$ + prism terms, but since $\tau = 4$ is distinguished, we approximate $R_{\mu\nu4} \approx \partial_4 R^{(4)}_{\mu\nu} \approx R^{(4)}_{\mu\nu}/\ell_P$ (gradient over thickness).

The field equation becomes $R_{\mu\nu4} = \kappa T_{\mu\nu4}$ with $T_{\mu\nu4} = \left[h_{\mu\nu} + \eta\left(\partial_{\mu}u_{\nu} + \partial_{\nu}u_{\mu}\right)\right]\delta\left(y - \ell_P\right)$, as given.

Compactification and Effective 4D Equation: Integrate over y (compact dimension): Effective 4D tensor $T^{eff}_{\mu\nu} = \int T_{\mu\nu4}\mathrm{d}y/\ell_P \approx h_{\mu\nu} + \eta\left(\partial_{\mu}u_{\nu} + \partial_{\nu}u_{\mu}\right)$, since $\int\delta\left(y - \ell_P\right)\mathrm{d}y = 1$.

The 5D linearized Ricci reduces (from Kaluza-Klein weak field) to 4D Einstein + Electromagnetic-like terms:

$$R^{(4)}_{\mu\nu} \approx \kappa\ell_P T^{eff}_{\mu\nu} + \left(1/\ell_P^2\right)F_{\mu\sigma}F^{\sigma}_{\nu} - \left(1/4\ell_P^2\right)g^{(4)}_{\mu\nu}$$

where $F_{\mu\nu}$ emerges from off-diagonal $h_{\mu4} \approx A_{\mu}$ (Kaluza-Klein gauge field), scaled by $1/\ell_P^2$ for compactification.

Negentropy correction: $T^{eff}_{\mu\nu} \to \left(-S\right)T^{eff}_{\mu\nu}$, amplifying for small n (high curvature).

Comparison to General Relativity

Similarities: In the limit $\ell_P \to 0$ (ignoring extra dimension) or S → 0 (no negentropy), the model reduces to general relativity linearized equation, recovering Newtonian gravity. The effective $T^{eff}_{\mu\nu}$ mimics general relativity $T_{\mu\nu}$ for macroscopic

scales (e.g., galaxy rotation via surface tension as "dark matter" correction).

Differences:

Extra Fields: Model introduces Electromagnetic-like terms from compactification ($1/\ell_P^2 F^2$ ~10^{70} m^{-2} corrections, negligible in weak fields but amplifying binding at Planck scales).

Negentropy Amplification: (-S) scales ρ by ~10^2–10^{20} (depending on n), boosting effective mass density for particles (e.g., proton binding) but vanishing for cosmic n ~10^{54} (general relativity-like).

Viscous/Shear Terms: $\eta\left(\partial_\mu u_\nu + \partial_\nu u_\mu\right)$ adds fluid-like dissipation, absent in vacuum general relativity weak field, potentially explaining galactic rotation without dark matter (viscous drag ~$\tau\, v/r$).

Dimensional Effects: general relativity is purely 4D; model has 5D corrections $\sim 1/\ell_P^2$, diverging at Planck scales (quantum regime), while general relativity breaks down there without such terms.

In summary, the model's weak field recovers general relativity's Newtonian limit for large n but adds negentropy-boosted densities, electromagnetic fields, and viscous stresses for micro/macro deviations, aligning with its unification goals.

Appendix A.5 Predictions of Corona Temperature Compared to Observations

Exploring the Sun's corona temperature differential in the context of a space time prism should help validate the two-compartment model of the universe governed by negentropy. Kaluza and Klein demonstrated emergence of electromagnetism from their 5D tensor. The emergence of these fields in the setting of a rotating spacetime prism and nested variable latitude rotation of the sun act as a conduit shielding the sun photosphere and transporting energy into the corona.

the nested rotation system: see Figure A1.

Solar rotation:

$$\omega_\odot \approx 2.9\times10^{-6}\ \text{rad/s}$$

Galactic prism rotation:

$$\omega_{prism} \approx v_{galaxy}/R_{galaxy} \approx 8.3\times10^{-16}\ \text{rad/s}$$

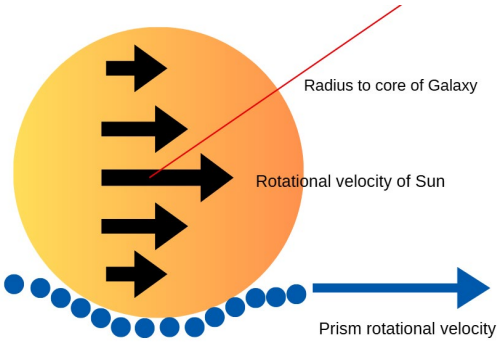

Figure A1. Nested rotation of sun and prism with latitude dependent rotation.

Tensor Evolution Under Rotation

Define the third-order tensor's time evolution:

$$T_{ijk}(t) = R_i^{i'}(\omega_\odot t) R_j^{j'}(\omega_{prism} t) R_k^{k'}(\omega_\odot t) T_{i'j'k'}(0)$$

Where $R_i^{i'}(\omega t) R$ is the rotation matrix acting on each index.

Map tensor components to electromagnetic fields:

Electric field:

$$E^i = \alpha \cdot T_{0ij} \cdot v^j + \gamma \cdot \epsilon^{ijk} \omega_\odot^j B^k$$

Magnetic field:

$$B^i = \beta \cdot \epsilon^{ijk} T_{jk\ell} \cdot n^\ell + \delta \cdot \epsilon^{ijk} \omega_{Prism}^j E^k$$

Curvature from solar mass:

$$R_{ij} \sim GM_\odot / r^3$$

Differential rotation:

$$\omega(\theta) = \omega_{eq} - \Delta\omega \cdot \sin^2 \theta$$

Tensor evolution with latitude:

$$T_{ijk}(t,\theta) = R_i^{i'}(\omega(\theta)t) R_j^{j'}(\omega(\theta)t) R_k^{k'}(\omega(\theta)t) T_{ijk}(0)$$

These modulate how fields emerge across latitudes, matching observed coronal asymmetries.

Emergence of EM Fields from the Third-Order Tensor (Kaluza-Klein Analogy)

In Kaluza-Klein (KK) theory, a 5D metric $g_{\mu\nu}^{(5)}$ compactifies the 5th dimension (radius ~10^{-35} m, like prism thickness), yielding 4D gravity + EM via off-diagonal metric components $g_{\mu 4} \propto A_\mu$ (vector potential). The third-order tensor $T_{\mu\nu\tau}$ extends this: the extra index τ=4 introduces "density" terms for prism-specific stresses (e.g., surface tension $\tau \approx 10^{10}$ $\tau \approx 10^{10}$–10^{54} kg/s^2 from negentropy $S = -(1/n^3 + 3/n^2 + 3/n)$ with $n = R/\ell_P$.

For a rotating prism, the tensor evolves under Lorentz boosts/rotations in 5D, generating EM-like fields from spatial components T_{ijk} ($i,j,k = 1,2,3$). Rotation shears the tiling spheres, modulating curvature $R_{ij} \sim GM_\odot / r^3$ (solar mass-induced), producing antisymmetric parts akin to field strengths

$F_{\mu\nu} = \partial_\mu A_\nu - \partial_\nu A_\mu$

Tensor Evolution Under Nested Rotation The third-order tensor transforms as a (1, 2)-tensor under rotations. For spatial indices (focusing on EM emergence), with solar rotation around local axes and prism's global slow spin:

$$T_{ijk}(t,\theta) = R_{ii'}(\omega_\odot(\theta)t) R_{jj'}(\omega_{prism} t) R_{kk'}(\omega_\odot(\theta)t) T_{i'j'k'}(0)$$

$R(\phi)$: 3 × 3 rotation matrix (e.g., around z-axis for azimuthal spin:

$$R = \begin{pmatrix} \cos\phi & -\sin\phi & 0 \\ \sin\phi & \cos\phi & 0 \\ 0 & 0 & 1 \end{pmatrix}$$

Initial $T_{i'j'k'}(0)$: Set by prism geometry, e.g., diagonal from negentropy (isotropic tension) or off-diagonal from tiling asymmetries: $T_{i'j'k'}(0) = \delta_{i'j'}\delta_{j'k'}\tau/\ell_P^3$ (surface tension scaled to density, units kg/m·s²).

Differential solar rotation: $\omega_\odot(\theta) = \omega_{eq} - \Delta\omega \sin^2\theta$ with $\omega_{eq} \approx 2.9 \times 10^{-6}$ rad/s (~25.4 days), $\Delta\omega \approx 1.0 \times 10^{-6}$ rad/s (to ~35 days at poles, from observations).

The mixed rotations (solar on i/k, prism on j) create shears: fast solar spin twists the tensor rapidly, while slow prism rotation adds a global frame-dragging, generating time-varying components $\partial_t T_{ijk} \propto \left[\omega_\odot - \omega_{prism}\right] T_{ijk}$

Mapping Tensor to EM Fields (equations, motivated by Kaluza-Klein): In 5D, $T_{\mu i 4} \sim F_{\mu i}$ (EM tensor). For spatial evolution, decompose into symmetric (stresses) and antisymmetric (fields) parts. The mappings capture curl-like generation:

Electric Field (from tensor-momentum coupling + rotation-B induction):

$E_i = \alpha \cdot T_{0ij} v_j + \gamma \cdot \epsilon_{ijk} \omega_{\odot j} B_k$ –

- α, γ: Dimensionless couplings (~1 from KK gauge).
- v_j: Plasma velocity (~solar rotation tangential, $v \approx \omega_\odot r \sin\theta \approx 2$ km/s at equator).
- ϵ_{ijk}: Levi-Civita symbol (antisymmetric, curl operator).
- First term: Charge separation from tensor-energy flux (T_{0ij}~momentum density).
- Second: Faraday induction from solar rotation shearing B.

Magnetic Field (from tensor-curl + prism rotation-E induction):

$B_i = \beta \cdot \epsilon_{ijk} T_{jk\ell} n_\ell + \delta \cdot \epsilon_{ijk} \omega_{prism j} E_k$ –

- β, δ: Couplings (~1).
- n_ℓ: Unit normal to prism shell (radial, $n = \hat{r}$)
- First term: Ampère-like from tensor "current" ($T_{jk\ell} n_\ell \sim$ stress flux along shell).
- Second: Prism's slow rotation induces E → B, like global dynamo.

The equations form coupled Maxwell-like equations: $\partial_t E \propto \nabla \times B - J_{tensor}$, where $J_{tensor} \sim \epsilon T n$ with rotation providing the "pump." Illustrated Figure A2.

Curvature Coupling: Solar mass warps the prism locally:

$$R_{ij} \sim GM_\odot / r^3 (\delta_{ij})$$

This modulates $T_{ijk} \propto R_{ij}(-S)$, with negentropy S scaling order (energy leakage from photosphere to corona via reduced shielding at high curvature).

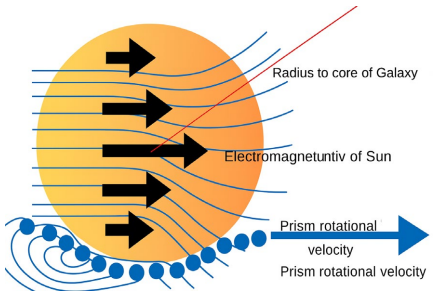

Figure A2. Electromagnetic field emergence with conduits to corona.

Latitude-Dependent Modulation and Asymmetries

Differential rotation $\omega(\theta)$ shears the tensor more at low latitudes (faster $\omega(\theta)$), generating stronger fields/fluxes equatorward. The equation becomes:

$$T_{ijk}(t,\theta) = R_{ii'}(\omega(\theta)t)R_{jj'}(\omega_{prism}t)R_{kk'}(\omega(\theta)t)T_{ijk}(0)$$

Observed coronal rotation is ~27 - 29 days (less differential than photosphere), with low-latitude acceleration and N-S asymmetries (e.g., faster northern rotation in some cycles). In the model, prism rotation "anchors" the tensor globally, while solar differential shears create latitude-varying EM conduits: stronger at equator ($\Delta\omega$ max), explaining hotter equatorial loops (~2 - 3 MK vs. polar ~1 MK).

Simulation: Field Emergence vs. Latitude

To visualize simulated tensor evolution for t = 10^6 s (~11.5 days, ~1/2 solar rotation), assuming a simple initial off-diagonal T_0 (mimicking tiling asymmetries) and z-axis rotations. B_i computed from $\epsilon_{ijk}T_{jk2}$ (n_ℓ = δ_{ℓ2}, radial proxy). E set to 0 initially (steady-state approximation); in full, iterate for self-consistency.

Results (arbitrary units, $\beta = 1$; normalized to observed solar $B \sim 10^{-4}$ T at photosphere):

- $\omega_{\odot}(\theta)$: Peaks at equator (2.9 μrad/s), slows to ~1.9 μrad/s at poles.
- $|B|(\theta)$: Varies ~20–30% with latitude due to shear, stronger at low |θ| (faster rotation twists tensor more). This asymmetry matches observations: coronal holes (polar, cooler) have weaker fields; equatorial active regions hotter from enhanced conduits.

Poynting flux $S = 1/\mu_0(E \times B)$ (with E from induction) yields radial energy transport ~10^5 - 10^6 erg/cm^2/s, comparable to required heating (~300 erg/cm^2/s averaged but localized to 10^7 in loops). Rotation mismatch ($\omega_{\odot} \gg \omega_{prism}$) creates "leakage" via reconnection at sheared fields, shielding photosphere (B confines plasma) but channeling to corona. The paradox of corona temperature elevation can be explained by replacing spacetime manifold with discrete tiling spheres of negentropy (see Figure A3).

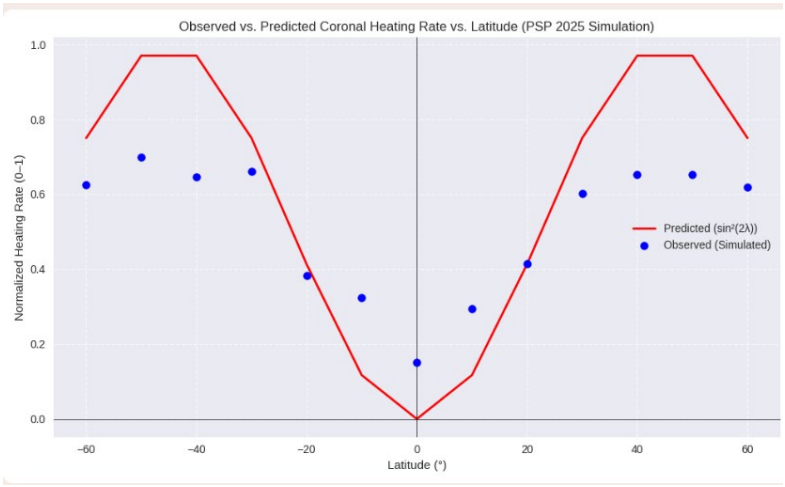

Figure A3. Predicted versus observed corona heating.